NUMERICAL STUDY OF A HEAT TRANSFER ACROSS A CONTACT PAIR

Yulia R. Kolosova[1], Aleksandr A. Dementiev[2], Aleksei I. Soldatov[1], Ahmed A. Abouellail[2], Andrei A. Soldatov[1]

[1] *Tomsk State University of Control Systems and Radioelectronics, Tomsk, Russia, soldatov.88@bk.ru*
[2] *National Research Tomsk State University, Tomsk, Russia, demo092@tpu.ru*

ABSTRACT

This paper is proposing a mathematical model for heat transfer distribution in the case of imperfect contact of two surfaces (an electrode and a sample), which allows one to obtain the temperature distribution in coupled bodies at any time – from the initial contact time to the establishment of the stationary mode.

Keywords: Contact thermal resistance, Non-destructive testing, Heat transfer

1. INTRODUCTION

Currently, the development of modern technology is accompanied by an intensive increase in thermal loads of components and structural parts due to an increase in the speed of machines, their power, productivity and accuracy. The thermal regime of components and parts is significantly affected by the thermal resistance of the contact due to the imperfection of the mechanical connection of the contacting surfaces. All materials and alloys used in the industry for manufacturing metal structures, metal structures themselves, and modern equipment are subject to input testing, i.e. the conformity of the sample to specified technical requirements (chemical composition, hardness measurement, etc.) is established. Even carefully machined hard metal surfaces are not absolutely smooth, they have a contact only in certain areas and have irregularities. To conduct a qualitative analysis of the test sample, there are thermoelectric control devices for the surface layer of the material or alloy (Abouellail *et al.*, 2017; Bahrami, 2005; Ciylan *et al.*, 2007; Carreon *et al.*, 2000). When there is a contact between an electrode heated to a certain temperature and a sample of a material or alloy, heat is transferred from the hot electrode to the sample and the thermoelectromotive force is measured. Each metal has unique thermoelectric properties, so by the magnitude of the thermoelectromotive force, the grade of steel or alloy can be determined.

Thermoelectric testing devices have a high measurement error, since the use of the point contact of the electrodes with the test sample does not allow obtaining high repeatability of the control results. The measurement error is affected by the force of pressing the electrodes to the test sample. If the force is insufficient for perfect point contact between the electrode and the test sample, then the heat from the hot electrode will not be transferred to the sample completely, part of the heat will be dissipated into the environment. An increased contact pressing of the electrode to the test sample can cause elastic and plastic deformations of the metal or alloy. In addition, the measurement error is affected by the presence of inhomogeneities in metals and alloys, the quality of the sample processing (surface roughness and heterogeneity, chips, cracks, shells, the presence of an oxide film, rust, the influence of heat treatment, etc.), the area and shape of the electrode contact, the presence of an intermediate layer (a liquid layer, etc.) on the surface of the test sample, as well as the probability of an accidental error associated with the human factor. To study the thermoelectric properties of metals and alloys during deformation, Thermo Fitness Testing, which is a device intended for the differential inspection of thermoelectric power, was developed at National Research Tomsk Polytechnic University (see Figure 1, Figure 2 for details) (Soldatov *et al.*, 2016). On the front panel the device has several service LEDs, a four-character seven-segment indicator and four buttons. The LEDs located to the left of the indicator and buttons serve to indicate the current operating mode of the device, while the LEDs located to the right of the indicator serve to record the measurement results. When working in a stand-alone mode, after switching it on, the device warms up for 10 minutes as the remote sensor is heating. A sign of the sensor warming is the blinking of the “Heating” LED. There are three levels of control, namely “normal”, “accurate” and “increased accuracy”. By default, the device is in the “normal” mode after being turned on. Switching between modes occurs by pressing the "Mode" buttons. If there is no contact between the sensor and the material being controlled, a “long minus” is displayed on the seven-segment indicators. As soon as the sensor contacts the material being controlled, the value of the difference between the thermoelectromotive force between the hot electrode and the test sample and the hot electrode and the material being controlled is displayed. However, it also has the disadvantages indicated above. Therefore, there is a need to provide a study investigating the influence of the thermal contact resistance on the process of heat transfer from the hot electrode to the test sample.

a *b*

Fig. 1. *a*) External appearance of the Thermo Fitness Testing device. *b*) The circuit of the test sample '*x*' relative to the standard '*e*', connected together and shorted by the thermoelectric sensor

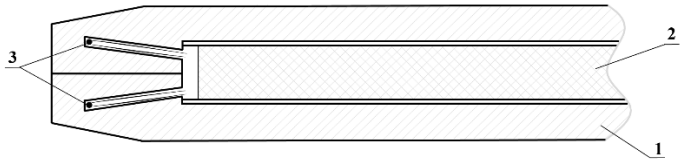

Fig. 2. The sensor design: 1 – hot electrode, 2 – heating element, 3 - thermocouples

The aim of the 09gastudy is to improve the quality of the thermoelectromotive force measurement with the Thermo Fitness Testing device, including analysis of the influence of measurement conditions (the force of pressing, the sample surface characteristics) on the temperature distribution in the zone of contact of the electrode with the test sample and refinement of the electrode geometry of the Thermo Fitness Testing device to control the thermoelectromotive force in accordance with the obtained research results that do not require the use of filled intercontact space.

2. MATHEMATICAL MODEL OF HEAT DISTRIBUTION IN THE CASE OF IMPERFECT CONTACT PAIR

There is a need for a numerical assessment of the influence of measurement conditions on the establishment of a stationary temperature distribution in the zone of contact between the electrode and the test sample during thermoelectric control. In order to reduce the error of thermoelectromotive force measurement, a one-dimensional mathematical model for heat distribution in the case of imperfect contact of two surfaces has been developed, which allows determining the temperature distribution in coupled bodies at any time – from the beginning of contact to the moment of reaching the stationary mode. An electrode with a height l_1 and an investigated sample with a height l_2 connected to each other were selected for the model. There is a gap d in the contact zone due to the roughness of the materials (see Figure 3 for details).

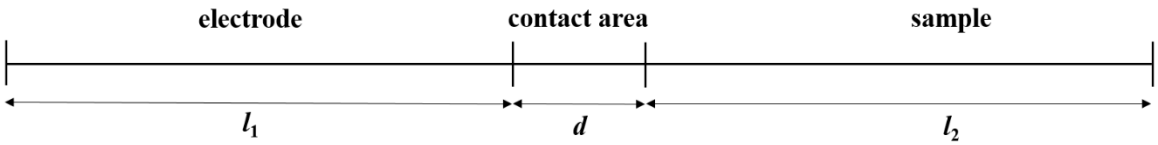

Fig. 3. Scope representation of an imperfect contact pair

The electrode heats the test sample, and the entire system is under normal atmospheric conditions and is cooled by natural convection.

The mathematical model in a dimensionless form for the electrode (1) and the test sample (2) can be written in the following way:

$$\frac{\partial \theta}{\partial \tau} = \frac{\partial^2 \theta}{\partial \xi^2} - H_1 Bi_1 \left(\theta - \frac{T_{air}}{T_{\max}} \right), \quad (1)$$

$$\frac{\partial\theta}{\partial\tau}=\frac{a_2}{a_1}\frac{\partial^2\theta}{\partial\xi^2}-H_2Bi_2\frac{a_2}{a_1}\left(\theta-\frac{T_{air}}{T_{\max}}\right), \quad (2)$$

where θ is the dimensionless temperature, τ is the grid time step, ξ is the dimensionless coordinate, $Bi_{1,2}$ is the Biot number that describes the ratio of the thermal resistance of a substance to the environment convection, $H_{1,2}$ is the doubled ratio of the length to the radius, T_{air} is the air temperature, $T_{\max}$ is the maximum temperature of the system, $a_{1,2}$ is the thermal diffusivity, an index of 1 refers to the electrode, an index of 2 refers to the test sample.

The initial conditions for the electrode and the test sample are presented in formulas (3-4):

$$\theta(\xi,0)=\frac{T_1}{T_{\max}},0\le\xi<\frac{l_1}{x^*}, \quad (3)$$

$$\theta(\xi,0)=\frac{T_2}{T_{\max}},\frac{l_1}{x^*}\le\xi<\frac{l_2}{x^*}, \quad (4)$$

where T_1 is the initial temperature of the electrode, T_2 is the initial temperature of the test sample.

The following scales were used to reduce the set of equations to a dimensionless form:

$x^*=l_1+l_2=l$ is the coordinate scale, $t^*=c_1\rho_1l^2/\lambda_1$ is the time scale, and $T_1=T_{\max}$ is the temperature scale.

At the left boundary of the computational domain, the first-order boundary condition is adopted (the temperature distribution on the surface of the body is specified) (5):

$$\theta\left(0,\tau\right)=\frac{T_1}{T_{\max}}, \quad (5)$$

At the right boundary, the third-kind boundary condition is adopted (it characterizes the law of heat transfer between the surface and the environment due to convection) (6):

$$\frac{\partial\theta}{\partial\xi}=-Bi_2\left(\theta(1,\tau)-\frac{T_{air}}{T_{\max}}\right), \quad (6)$$

The heat transfers at the interface between the electrode and the test sample is described by the fourth-kind boundary conditions (the equality of temperatures and heat fluxes is specified). If there is a gap in the form of roughness of the materials, the boundary conditions at the contact interface between the materials are written in the form (7):

$$\frac{\lambda_1}{h}\left(\frac{\partial\theta}{\partial\xi}\left(\frac{l_1^-}{x^*},\tau\right)\right)=\frac{1}{R_{TCR}}\left(\frac{\partial\theta}{\partial\xi}\left(\frac{l_1}{x^*},\tau\right)\right),\quad \frac{1}{R_{TCR}}\left(\frac{\partial\theta}{\partial\xi}\left(\frac{l_1^+}{x^*},\tau\right)\right)=\frac{\lambda_2}{h}\left(\frac{\partial\theta}{\partial\xi}\left(\frac{l_1}{x^*},\tau\right)\right) \quad (7)$$

where λ_1, λ_2 are the coefficients of thermal conductivity of the electrode and the test sample, R_{TCR} is the thermal contact resistance.

3. THE METHOD OF CALCULATING THE THERMAL CONTACT RESISTANCE

Solids touch each other only with the vertices of the roughness profiles. Contact thermal resistance arises at the interface and physical contacts are limited by a finite number of separated points at the interface. Due to the presence of microroughness on the bonded flat surfaces, their contact is discrete. The actual contact area is on a microscopic scale, it is relatively very small compared to the visible contact area. (Mantelli *et al.*, 2003). Thus, due to the presence of the contact gap, the path length of the heat flux is significantly increased. The heat flux lines are brought together in stages: first, within the nominal cross sections, the heat flux lines are pulled together to contact macrospots caused by waviness, and then within each macrospot – to microspots due to roughness. There is a curvature of isothermal surfaces during thermal contact of solids. The heat transfer through connected solid materials is a complex process, depending on many geometric, thermal, and mechanical parameters, such as the geometry of the contacting solids, the thickness of the gap, the thermal conductivity of the contacting solids, the hardness and elastic modulus of the contacting solids, the average temperature of the interface, etc. The total thermal resistance of the contact is determined by the purity of the treatment, the load, the thermal conductivity of the medium, the thermal conductivity of the materials of the contacting parts, and other factors.

Currently, a large number of works have been devoted to contact heat transfer (Bahrami *et al.*, 2005; Tomimura *et al.*, 1995; Makhlouf *et al.*, 2014; Carreon, 2002; Stuart, 1987).

Heat transfer through the contact zone is accompanied by a drop in temperature ΔT, which depends on the heat flux density. Since the heat flux bifurcates when approaching the contact surface, it is reasonable to connect the value of the total contact thermal resistance with two components, namely the resistance of the intercontact medium R_s and the resistance of the actual contact R_c, which act in parallel. Then, according to the rule of addition of parallel resistances, they can be written in the following way:

$$R_{TCR} = \frac{1}{R_C} + \frac{1}{R_s}, \tag{8}$$

The temperature field distribution can be represented as a one-dimensional line on the contact surfaces, as shown in Figure 4 (Mantelli *et al.*, 2003).

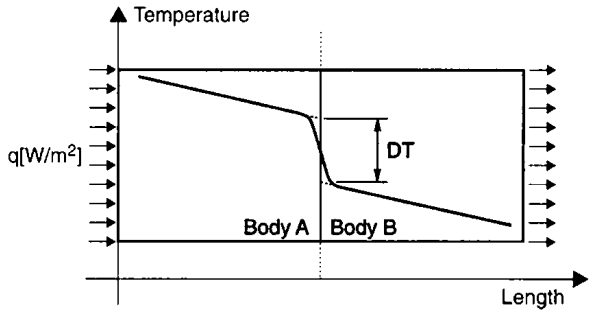

Fig. 4. Temperature drop in the place of imperfect contact materials

Table 1 presents the result of calculating the thermal contact resistance R_c depending on the pressure P, the degree of roughness R_z, the roughness W_z, and the investigated materials steel St20 according to the calculated dependences proposed by authors (Marotta *et al.*, 2001).

Table 1. Contact thermal resistance R_c depending on pressure and surface roughness.

P, KPa	$R_c \cdot 10^{-4}$, m²· K/ W		
	at R_z=1 μm and W_z=20 μm	at R_z=1,5 μm and W_z=50 μm	at R_z=2 μm and W_z=100 μm
1	2,06	3,54	5,25
2	1,52	2,57	3,76
3	1,2	2,11	3,09
4	1,1	1,84	2,68
5	0,99	1,65	2,4
6	0,91	1,51	2,19

From Table 1 it is seen that:

1. With an increase in the load acting on the test samples, the total contact thermal resistance decreases.
2. The higher the roughness, the more significant the contact thermal resistance.

4. NUMERICAL STUDY ON THE MATHEMATICAL MODEL FOR UNSTEADY HEAT DISTRIBUTION

Based on the foregoing, a one-dimensional mathematical model for the unsteady heat distribution was developed; the study was carried out in the case of an imperfect pressing of the electrode to the test sample. The values of the thermo-physical characteristics of steel St20 were taken from the reference data. The results of numerical simulation for a one-dimensional mathematical model of unsteady heat distribution in the case of an imperfect pressing of the electrode to the test sample are presented in Figures 5 to 7.

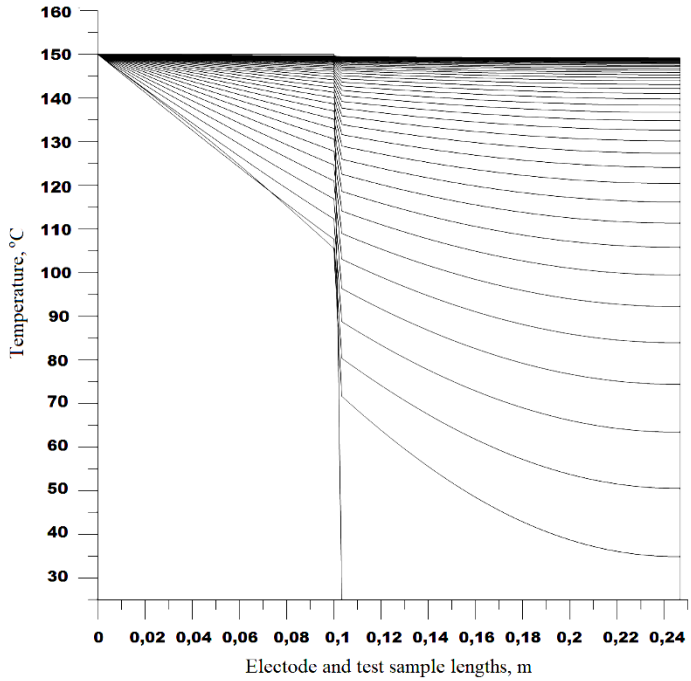

Fig. 5. Distribution of the temperature field in the case of an imperfect pressing of the electrode to the test sample, at the time step Δ*t* at various points in time: *1*– $t=t_0$; *2*- $t=t_0+\Delta t$, …, *n*- $t=t_0+n\Delta t$ R_c=2,19·10^{-4}, m^2· K/ W, R_z=2 µm and W_z=100 µm

At the initial time t = 0, the initial conditions are implied. Further, due to thermal conductivity, heat exchange occurs between the hot electrode and the sample through the non-contact zone. Over time, the temperature difference decreases, the temperature field is established and the stationary distribution takes the form of a straight line. The simulation showed that with the initial data, the temperature of the system decreases from 150 to 149 °C, that leads to a corresponding decrease in the thermoelectromotive force, which is directly proportional to the temperature (see Figures 5, 6 for details).

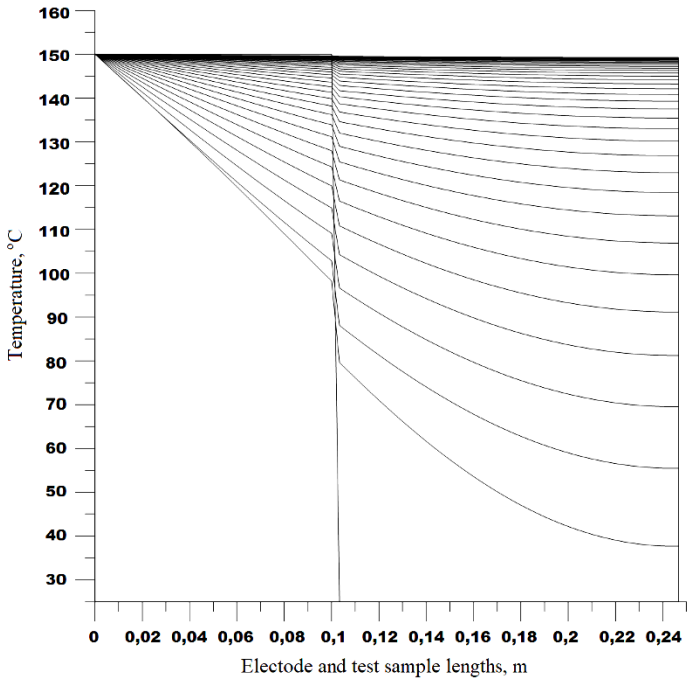

Fig. 6. Distribution of the temperature field in the case of an imperfect pressing of the electrode to the test sample, at the time step Δ*t* at various points in time: *1*– $t=t_0$; *2*- $t=t_0+\Delta t$, …, *n*- $t=t_0+n\Delta t$ R_c=1,54 ·10^{-4}, m^2· K/ W, R_z=1,5 µm и W_z=50 µm

A parametric study was carried out on the influence of the percentage of the contact area on the time of the stationary regime at the boundary of the gap and the test sample (see Figure 7 for details). It can be seen that at η = 1 % the time in the stationary mode is five times longer than at η = 10 %. This is due to the fact that the value of thermal contact resistance in the gap is less. This means that the better the surfaces of a metal are treated, the faster the heat flux will be established.

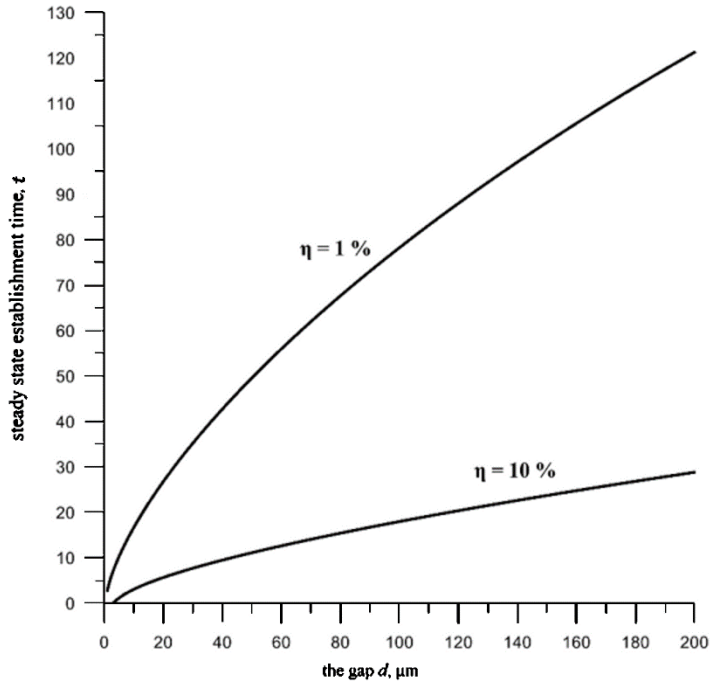

Fig. 7. The effect of gap *d* on establishment time *t* of stationary heat flow

Verification of the developed mathematical model was carried out using a commercial software package using the finite element method. This technique is applicable to evaluate the temperature conditions of materials for conducting research on contact thermal resistance of contact pairs.

5. CONCLUSIONS

A mathematical model of heat distribution has been developed in the case of the presence of two surfaces (a system – an electrode), depending on the degree of roughness and unevenness of its own surfaces, which allows obtaining temperature data for a fixed time to reach the steady state heat flux.

To further improve the quality of measuring the thermoelectromotive force of the device, it is necessary:

1. to model the contact of the roughness of the interacting surfaces to take into account the geometric features of the electrode, as well as to conduct experimental studies to test the results of a numerical study.

2. to develop a scientific and methodological basis for experimentally determining the time of reaching the stationary mode of thermal contact of the system (electrode-sample) and calculating the thermoelectromotive force.

3. to obtain a pattern of change in the value of the contact thermal resistance parameter depending on the degree of roughness and unevenness of the material or alloy, which is still under study.

REFERENCES

Abouellail, A.A., Obach, I.I., Soldatov, A.A., and Soldatov, A.I. (2017). Surface inspection problems in thermoelectric testing, *MATEC Web Conference*, 102, ID 1001, 1-4.

Bahrami, M., Yovanovich, M., and Culham, J. (2005). Thermal contact resistance at low contact pressure: Effect of elastic deformation, *J. heat mass Transf.*, 48(16), 3284-3293.

Carreon, H., Nagy, P.B., and Nayfeh, A.H. (2000). Thermoelectric detection of spherical tin inclusions in copper by magnetic sensing, *Journal of Applied Physics,* 88(11), 6495.

Carreon, H. (2002). Thermoelectric Nondestructive Evaluation of Residual Stress in Shot-Peened Metals, *Res. Nondestruct. Eval.,* 14(2), 59.

Ciylan, B., and Yılmaz, S. (2007). Design of a thermoelectric module test system using a novel test method, *Int. J. Therm. Sci.*, 46(7), 717-725.

Hu, J., and Nagy, P.B. (1999). On the Thermoelectric Effect of Interface Imperfections, in: Review of Progress in Quantitative Nondestructive Evaluation, 18B, *Springer, Boston, MA*, 1487-1494.

Hu, J., and Nagy, P.B. (1998). On the role of interface imperfections in thermoelectric nondestructive materials characterization, *Appl. Phys. Lett.*, 7(4), 467.

Kikuchi, M. (2010). Dental alloy sorting by the thermoelectric method, *Eur. J. Dent.*, 4(1), 66-70.

Li, J.F., Liu, W.S., Zhao, L.D., and Zhou, M. (2010). High-performance nanostructured thermoelectric materials, *Npg Asia Mater.*, 2(4), 152.

Marotta, E.E., Fletcher, L.S., and Dietz, T.A. (2001). Thermal Contact Resistance Modeling of Non-Flat, Roughened Surfaces With Non-Metallic Coatings. *Journal of Heat Transfer*, 123(1), 11-23.

Makhlouf, M., and Chadouli, R. (2014). Modeling of the thermal contact resistance of a solid-solid contact. *IOSR Journal of Mechanical and Civil Engineering (IOSR-JMCE),* 11(5), 72-82.

Mantelli, M.B.H., and Yovanovich, M.M. (2003). Thermal contact resistance. Spacecraft Thermal Control Handbook, *CA: Aerospace*, 1, 599-637.

Nagy, P.B. (2010). Non-destructive methods for materials' state awareness monitoring, *Insight: Non-Destructive Testing and Condition Monitoring*, 52(2), 61.

Soldatov, A.I., Soldatov, A.A., Sorokin, P.V., Loginov, E.L., Abouellail, A.A., Kozhemyak, O.A., and Bortalevich, S.I. (2016). Control system for device «thermotest», In: *International Siberian Conference on Control and Communications (SIBCON)*, 1-5.

Stuart, C. (1987). Thermoelectric Differences Used for Metal Sorting, *J. Test. Eval.*, 15, 224-230.

Stuart, C.M. (1983). The Seebeck effect as used for the nondestructive evaluation of metals, *Int. Adv. Nondestr. Test.,* 9.

Ritzer, T.M., Lau, P.G., and Bogard, A.D. (1997). A critical evaluation of today's thermoelectric modules, Thermoelectrics. *Proceedings ICT '97*, 619-623.

Tomimura, T., Fujii, M., Kawamura, Y., Sakugawa, J., and Kurozumi, T. (1995). Mean Thermal Contact Resistance of Wavy Solid Surfaces, *Kyushu University*, 9(1).